IFSA 2005, Industrial Fluidization South Africa: pp. 345–355. Edited by A. Luckos and P. Smit
Johannesburg: South African Institute of Mining and Metallurgy, 2005

A study into the hydrodynamic behaviour of heavy minerals in a circulating fluidized bed

A. Luckos and P. den Hoed
MINTEK, Randburg, South Africa

Keywords: fluidization, hydrodynamics, heavy minerals, circulating fluidized bed, pressure profiles, slip velocity, L-valve

Abstract—To understand the hydrodynamic behaviour of titania-bearing solids undergoing chlorination in CFB reactor at 1000°C, tests were conducted in a Perspex replica of the CFB. The cold model stands 5-m tall; the internal diameter of the riser is 80 mm. Circulating solids in the CFB return to the riser through an L-valve. Four materials were tested, three of them heavy minerals (ilmenite, rutile and titania slag); the fourth, silica sand. Superficial gas velocities were run at values of 2.8–7.4 m/s; solids-circulation fluxes, at values of 5.3–75 kg/m^2·s. At fixed gas velocities, increasing rates of solids circulation increased both the average pressure at each point in the CFB and the pressure gradients at the top and bottom of the riser. At constant rates of solids circulation, increasing gas velocities raised the average pressure at each point in the CFB, but decreased the pressure gradient in the lower sections of the riser. Solids concentrations were higher at the top and bottom of the riser than they are half way up.

Slip velocities between the gas and particles in the riser ranged from 4 to 11 times the terminal velocities of single particles. The dimensionless slip velocity, U_{sl}/U_t, was independent of the solids-circulation flux. U_{sl}/U_t, correlates linearly with the dimensionless velocity, U/U_t. The solids-circulation flux through the L-valve correlated independently with pressure drop across the valve and with superficial aeration velocity. The study answered puzzling questions about the operation of the CFB chlorinator.

INTRODUCTION

Titanium tetrachloride is a valuable precursor to titania (TiO_2) pigments and titanium metal. It is produced commercially by chlorinating titaniferous ores and slag in bubbling fluidized beds (BFB) at high temperature. The process is established and profitable in developed countries. South Africa does not run a chloride process, yet it produces a quarter of the world's titaniferous raw materials. As a hopeful step in redressing the balance MINTEK recently designed, built and commissioned a pilot facility for producing $TiCl_4$.[1] The design was that of a circulating fluidized bed, a choice made to take advantage of certain benefits: a CFB chlorinator—so it was argued—would run at higher levels of productivity, could treat finer (sulfate-grade) slag, and could tolerate more alkaline-earth elements without defluidizing.[2] Estimates showed the concept to be as profitable as the conventional BFB process. To contain a corrosive chlorine at 1000°C the design included an L-valve and called for graphite as the material of construction, but it lacked instruments such as pressure sensors, which can be used to monitor the flow of solids in a CFB. Unable to observe the internal dynamics of our reactor, we built a replica, a cold model, of the CFB. Understanding the hydrodynamics of solids in the cold model, we reasoned, would help us to run the chlorinator effectively.

Our study served two purposes. First, it showed up conditions that could affect the kinetics of chlorination. In fluidized systems gas-solid interactions influence rates of heat and mass transfer, which in turn may speed up or slow down rates of reaction, and raise or lower the conversion of reactants. Three conditions bear particular consideration. The fraction of solids in

sections of the riser is one of them, for as the chlorination reaction involves the movement of gaseous species between particles of oxide and reductant (coke), so high concentrations of solids are less likely to hinder the reaction.[3] Another condition is the holdup of solids in the riser; it relates to residence time and, therefore, conversion. The third condition is slip velocity: the greater the slip, the higher rates of heat and mass transfer are likely to be.

Developing useful correlations between process variables is the second purpose served by this study. Such correlations can be used (1) for modelling the chemical and physical processes in the CFB, and (2) for developing a PLC control strategy to operate a CFB reactor in industry. As published correlations—many of them derived for coarse silica sand (Group B) and fine FCC (Group A in Geldart's classification)—substantially underestimated operating conditions in the cold model, we developed our own for fine, dense materials in circulation.

This paper considers three aspects of the hydrodynamic behaviour of heavy minerals in the CFB at MINTEK. First, it presents profiles of pressure and solids concentration in the unit. Secondly, it describes slip velocities in the upwardly flowing stream of the riser. As Davidson showed,[4] the average slip velocity—the difference between the mean interstitial velocity of the gas and the mean upward particle velocity—is given by

$$U_{sl} = \frac{U}{\varepsilon} - \frac{G_s}{\rho_p(1-\varepsilon)} \qquad (1)$$

Values of U_{sl} are usually higher than the terminal velocity, U_t of a single particle because "particles form aggregates, which can fall through the gas at velocities much higher than the free-falling velocity of one particle."[4] The aggregates take two forms; there are (1) relatively large, dense clusters of particles, and (2) films of particles falling near the wall of the riser, part of a phenomenon called core-annulus flow.[4]

The operation of the L-valve is the third aspect of hydrodynamics described in this paper. The L-valve is a non-mechanical device for controlling solids flow in CFBs. Because it has no moving parts in contact with solids, it is well suited to use in corrosive environments at high temperature. The device allows one to measure solids-circulation flux, G_s, an important variable that is otherwise difficult to measure. It does so indirectly through correlations, one of them between G_s and U_a, the superficial aeration velocity; the other between G_s and ΔP_v, the pressure drop across the L-valve. As the aeration flow is easily controlled, so values of U_a and ΔP_v are readily known. Our understanding of the hydrodynamics in the CFB cold model answered questions about the operation and performance of the CFB chlorinator.

TEST PROCEDURE

Tests were conducted in a CFB unit of transparent PVC (Figure 1). The riser column stands 5-m tall; it has an internal diameter of 80 mm. The distributor at the base of the column is a composite, a perforated plate over fine (106-µm) mesh. Circulating solids pass through a right-angled bend at the top of the column, into a cyclone, down a standpipe, and through an L-valve, which meets the riser 100 mm above the distributor (*i.e.,* from the centre line of the horizontal leg of the L-valve). The internal diameter of the standpipe and L-valve is 50 mm. Aeration (for circulation) is supplied at the base of the standpipe, 100 mm above the centre line of the horizontal leg. Pressure transducers, located at intervals up the riser, measure gauge pressure. A data-acquisition unit records the signals from the transducers. The apparatus is described in more detail elsewhere.[5]

MATERIALS TESTED

Tests were conducted with four materials of different type: silica sand, concentrates of rutile (nominally TiO_2) and ilmenite ($FeTiO_3$), and titania slag (nominally 86% TiO_2). Rutile and ilmenite are heavy minerals (specific gravity >2.9), although titaniferous slag, which is synthetic—being produced from ilmenite by smelting and crushing to size—may be classed as heavy, too (see Table 1). The sample of silica is river sand, milled and screened. The two concentrates derive from beach-sand deposits on the coast of South Africa. Particles in the formation of these deposits were smoothed and rounded (see Figure 2). By contrast, the samples of silica and slag were crushed to size. Their particles are irregular, and surfaces are angular (*i.e.,* sharp edged). The two contrasts in shape are captured in a dimensionless measure

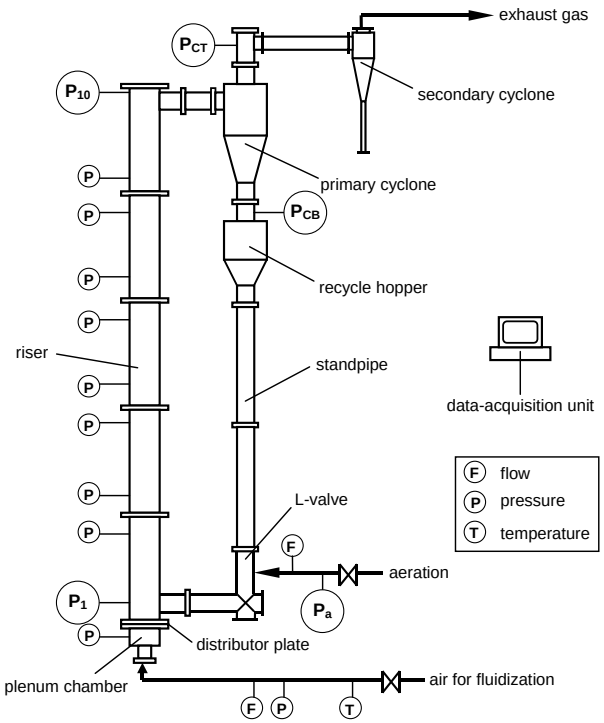

Figure 1. Schematic diagram of the CFB unit

called sphericity (Table 1), which relates the surface of a particle to the surface of a sphere of equal volume. The more spherical a particle, the closer ϕ_s is to 1.

We estimated the sphericity of particles in a sample from polished sections through particles (using image analysis).[6] The estimate is approximate, for it translates the area and perimeter of a section through a particle to the volume and surface area of that particle, by no means a straight-forward relationship in irregular particles. Sphericity as a measure of shape is problematic in another respect: an infinite number of different shapes (*e.g.*, cube, polygon or needle) can yield identical values of sphericity. Nevertheless, until a better measure of shape is devised, sphericity as defined is a working measure at least, and the best measure that we have. Capturing the irregular shapes of particles and the angular nature of their surfaces by a useful measure is a matter that needs revisiting. Until we do so, we may find anomalies in the pattern of hydrodynamic behaviour of materials with differently shaped particles.

The samples fall into Group B of Geldart's classification,[7] which means that the bed of particles fluidizes well, and collapses as soon as the flow of fluidizing gas is stopped.

Table 1. Physical properties of the materials tested

Property	Silica	Rutile	Ilmenite	Slag
Size range, μm ($_{20}d_{80}$)	70–440	80–165	55–120	70–330
Surface-volume mean diameter, μm	190	115	80	155
Particle density, kg / m^3	2660	4085	4710	4000
Bulk density, kg / m^3	1246	2337	2605	1912
Voidage of the fixed bed	0.53	0.43	0.45	0.52
Sphericity†	0.7	0.8	0.8	0.5
Minimum fluidizing velocity, m / s	0.031	0.020	0.011	0.030
Particle terminal velocity, m / s	1.08	0.89	0.59	1.02
Archimedes number at 25ºC	624	212	82	509

† The value for silica sand is taken from Kunii & Levenspiel (1991)[8]

TEST PROCEDURE

Tests on the four materials were conducted at a number of superficial gas velocities, U, and solid mass fluxes, G_s, a variable controlled partly by the aeration flow rate. The superficial gas velocity was set at values of 2.8–7.4 m / s; the solids-circulation flux, at values of 5.3–75 kg / m^{2}·s. Table 2 summarizes settings of the aeration velocity. Measurements were taken at each setting of the control variables: pressures in the loop of the CFB, the rate at which the bed moved down the standpipe, and the level of the moving bed in the standpipe were recorded at intervals of several seconds. For each set of data collected averages were calculated for periods of 2–5 minutes of steady operation. The pressure-drop profile along the riser and the pressure drop across the L-valve were calculated from these pressure measurements.

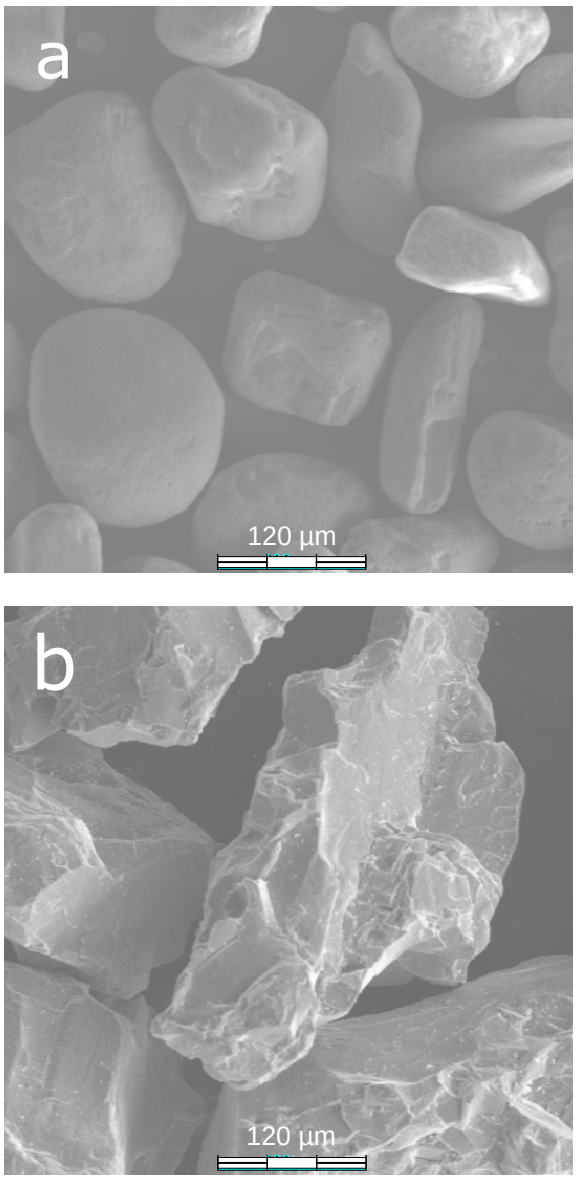

Figure 2. Secondary-electron images of particles of (a) rutile and (b) slag

The solids concentration, C_s, in any section of the riser is related to the pressure drop across that section:

$$\frac{\Delta P}{\Delta z g} = \rho_p (1 - \varepsilon) = C_s \qquad (2)$$

Equation 2 neglects pressure losses due to particle acceleration and to friction between gas or solids and the riser wall. These losses are comparatively small.

RESULTS

Profiles of pressure and concentration

The profiles of pressure in the unit map out a loop that is characteristic of CFBs (see figures 3 and 4). The profiles for all materials change in a regular fashion. At a fixed gas velocity, U, increasing rates of solids circulation, G_s, increase both the average pressure at each point in the CFB and the pressure gradient in the lower and upper sections of the riser (Figure 3). When the solids-circulation rate is held constant and the superficial gas velocity increased, the average pressure at each point in the CFB rises, but the pressure gradients in the lower sections of the riser decrease (Figure 4). As equation 1 relates, steep pressure gradients correspond to high solids concentrations (see figures 5 and 6). These profiles are generally C-shaped. Solids concentrations are high towards the ends of the riser: in the lower part, because particles accumulate in what is left of a fluidized bed; and in the upper part, because particles rebound from the plate closing the top of the column. Decreasing the solids-circulation rate lowers the solids concentration at each point in the riser (Figure 5). Increasing the superficial gas velocity at constant solids-circulation flux does likewise, except for the section at the top of the riser. In this section the flow of solids is constrained by the sharp elbow of the riser exit (Figure 6). Decreasing the solids-circulation flux or increasing the superficial gas velocity lowers the concentration of solids in the lower sections of the riser. As one continues the trend the solids concentration approaches the concentration higher up in the column, and the mode of fluidization is said to approach that of pneumatic transport.

Table 2. Superficial velocities of aeration gas, m / s

Rutile	0.02–0.07
Ilmenite	0.03–0.09
Silica sand	0.03–0.09
Titania slag	0.08–0.12

These patterns are repeated for all the materials tested. There are small differences in detail: (1) coarser particles (slag) appear to produce higher solids fractions than do finer particles (rutile), (2) the rebound zone at the top of the column is longer for denser particles, and (3) denser particles produce higher solids fractions in the upper sections than those of less-dense particles (an effect attributed to the greater kinetic energy of denser particles). [5]

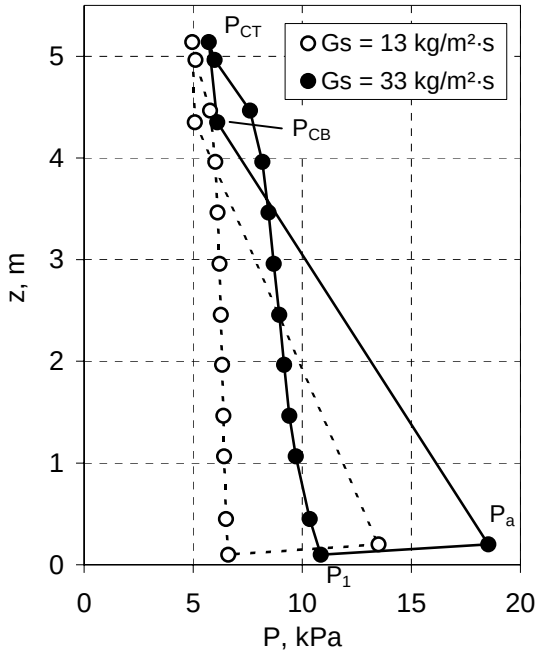

Figure 3. Pressures in the loop of the CFB as a function of G_s; for rutile at U = 4.9 m / s

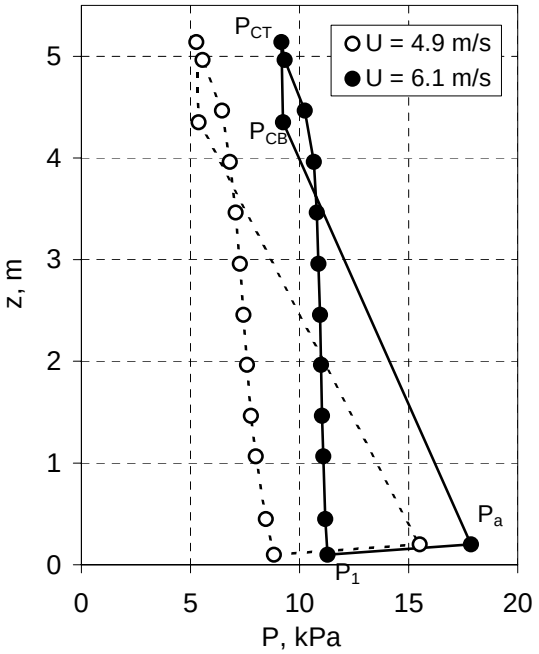

Figure 4. Pressures in the loop of the CFB as a function of U; for slag at G_s = 24.5 kg / m²·s

Slip Velocity

As expected, average slip velocities, U_{sl}, are higher than the terminal velocities, U_t, of single particles: indeed, slip velocities range from 4 to 11 times the terminal velocities of particles (see figures 7 and 8). Our observations show the dimensionless slip velocity to be independent of G_s at a fixed superficial gas velocity, a result that contradicts those obtained with FCC particles.[9] Yerushalmi and Avidan showed the slip velocity of FCC particles—which fall into Group A of Geldart's classification—to be a strong function of G_s at any superficial gas velocity.[9] Smolders and Baeyens tested small, rounded sand particles and found a similar trend.[10]

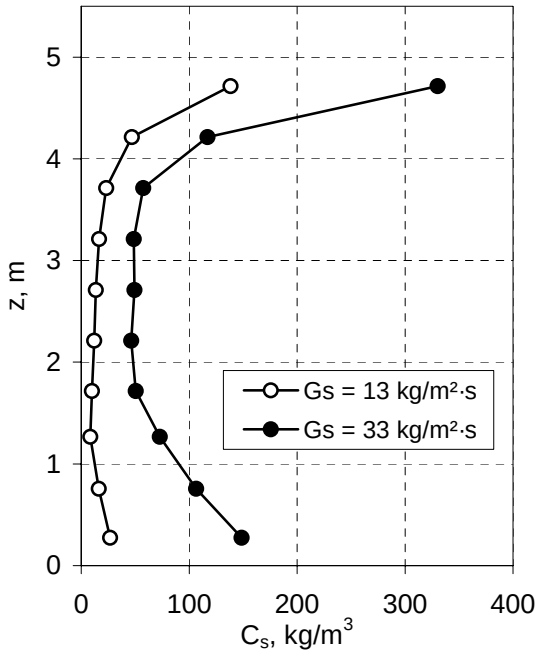

Figure 5. Profiles of solids concentration in the riser for rutile at fixed U

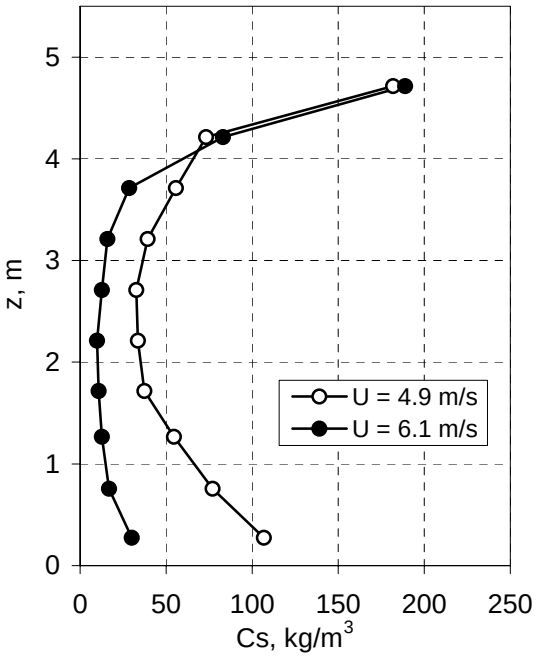

Figure 6. Profiles of solids concentration in the riser for slag at fixed G_s

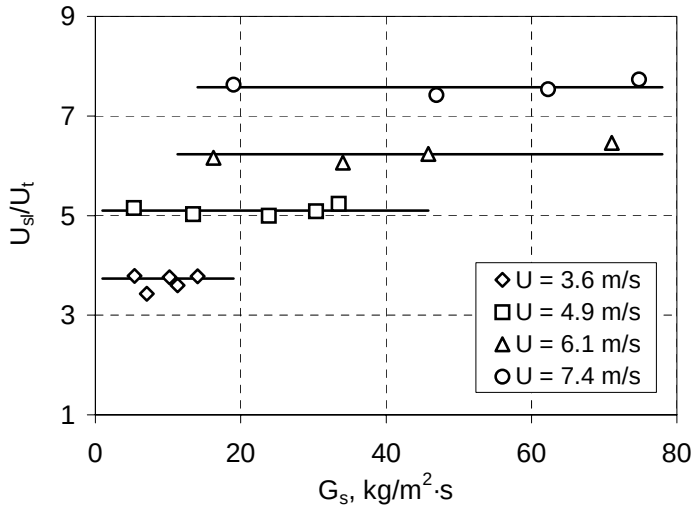

Figure 7. Dimensionless average slip velocities for rutile

Relationships are simple in other respects. The average slip velocity is proportional to the superficial gas velocity, and appears to increase with the density of the material (see Figure 9). When the (dimensionless) superficial gas velocity is expressed as a ratio of the terminal velocity of each material, the dimensionless average slip velocities for the four materials appear to conflate into a single line (see Figure 10). The relationship can be represented by

$$\frac{U_{sl}}{U} = 0.939\frac{U}{U_t} - 0.134 \qquad (3)$$

All experimental values of the dimensionless average slip velocity fall within 13% of values calculated by equation (3); the average deviation is 4.7%.

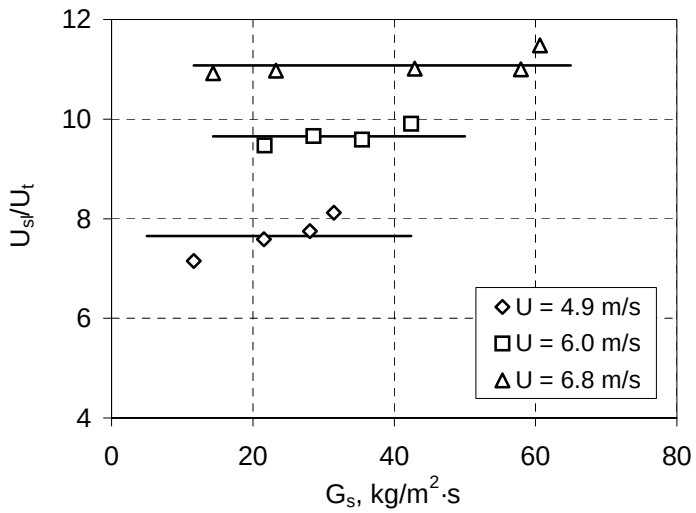

Figure 8. Dimensionless average slip velocities for ilmenite

L-valve Operation

The operation characteristic of L-valves can be described by a relationship between the rate of solids flow through the valve and the aeration-gas flow rate. The relationship is generally linear, but it is not unique: it differs from one material to the next (*i.e.*, materials of different particle size, density, and sphericity—see Figure 11). In the past two decades at least two studies have modelled the relationship, bringing in the diameter of the L-valve, D_v, and the minimum fluidizing velocity, U_{mf}, for the material tested. Figure 12 presents three expressions of the relationship in the variables of the published models—one expression treats two of the materials, and there is an expression each for slag and ilmenite. Of the published models, Geldart and Jones found that[11]

$$\frac{G_{sv}}{D_v} = 3354\frac{U_a}{U_{mf}} - 2965 \qquad (4)$$

The equation underestimates significantly our observations. Smolders and Baeyens introduced particle size into the equation,[10]

$$\frac{G_{sv}}{D_v} = 79600\left(\frac{U_a}{U_{mf}}\right)^2 d_p^{0.6} \qquad (5)$$

and found the relationship to assume a quadratic form. The equation also underestimates our observations, but less so than that of Geldart and Jones.[11] To correlate more accurately our observations of solids flow through the L-valve with the aeration flow rate we introduced two

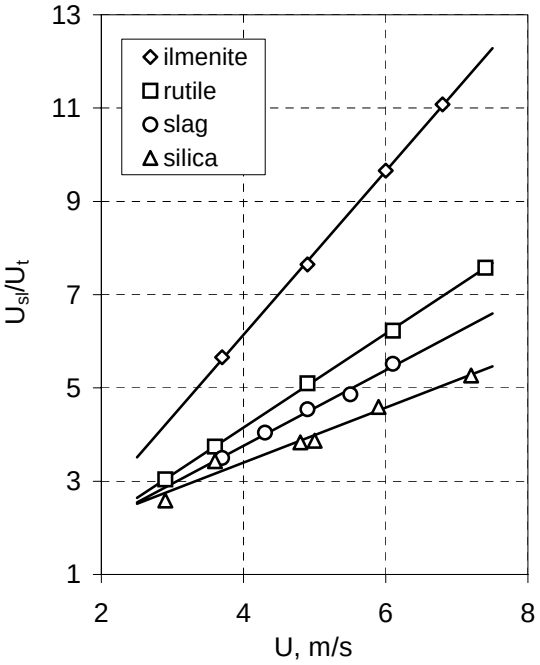

Figure 9. Dimensionless slip velocities for different materials

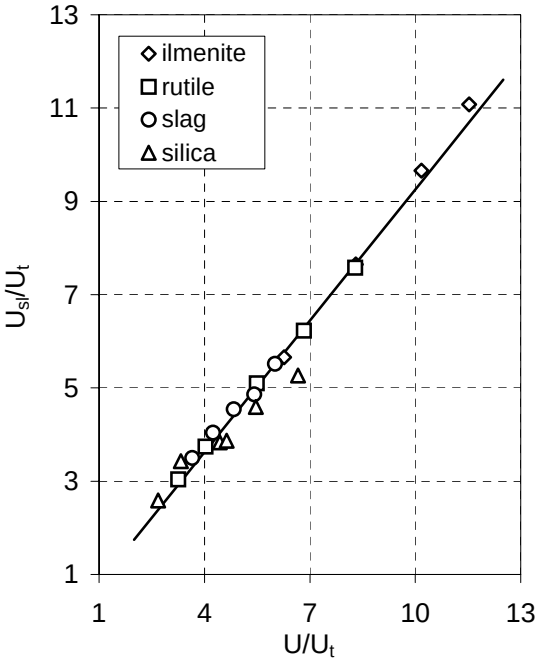

Figure 10. Relationship between dimensionless velocities—slip and superficial gas

further variables, solids density—captured in the dimensionless Archimedes number—and sphericity. We found that

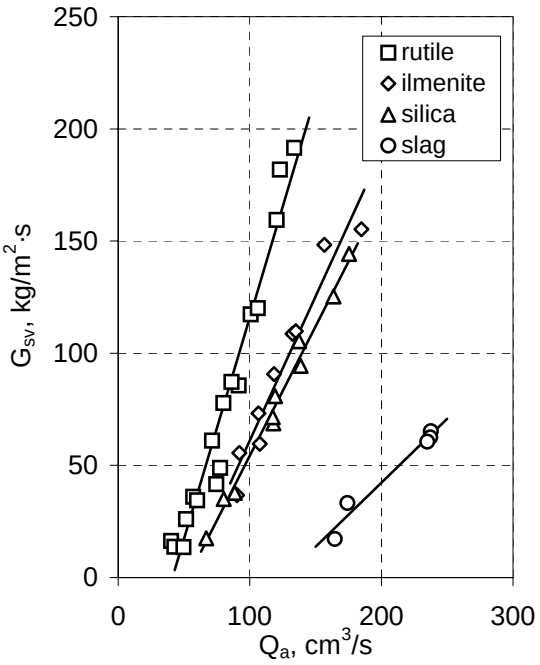

Figure 11. Proportionality between solids flow through the L-valve and the aeration flow rate

$$\frac{G_{sv}}{D_v} = 1.758\left(\frac{U_a}{U_{mf}}\right)^{1.95} Ar^{1.27}\phi_s^{6.9} \qquad (6)$$

The correlation coefficient is 0.94, and the average deviation between the correlation and the experimental data is ~20% (see Figure 13). We make the following inferences from equation 6: the correlation suggests (1) a dependence between G_{sv} and U_a that, as Smolders and Baeyens found,[10] is quadratic, and (2) a strong dependence of G_{sv} on the shape of the particles. Using the aeration flow to control solids flow in the L-valve as set out in equation 6 remains problematic, however; for the relationship depends on a variable—sphericity—that is not readily quantified accurately.

A handle on the control of solids circulation in a CFB is suggested by an analogy. Pressure drops across an L-valve is analogous to pressure drops across a slide valve, which Jones and Davidson,[12] treating the fluidized solids as an inviscid liquid, characterized as

$$\Delta P_v = \frac{1}{2\rho_p\left(1-\varepsilon_{mf}\right)}\left[\frac{W_s}{C_D A_v}\right]^2 \tag{7}$$

The opening, A_v, and discharge coefficient, C_D, of a mechanical valve are known; and, if the bulk density at minimum fluidization is known, equation 7 is sufficient to relate the flow of solids to the pressure drop across the valve.[13] In L-valves, however, the opening is both unknown and dependent on the aeration rate. (The valve openings in the tests we conducted were variable and small; a packed bed obstructed much of the cross-sectional area at the elbow of L-valve.) Despite being not readily quantified from first principles in L-valves, a dependence between ΔP_v and W_s in equation 7 nevertheless underpins relationships developed in two studies. Geldart and Jones correlated the two variables along with a physical property of the material and two conditions of geometry:[11]

$$\frac{\Delta P_v}{L_v} = 0.216\frac{G_{sv}^{0.17}}{D_v^{0.63} d_p^{0.16}} \tag{8}$$

Arena and co-workers developed a correlation of similar form, but added into the equation the

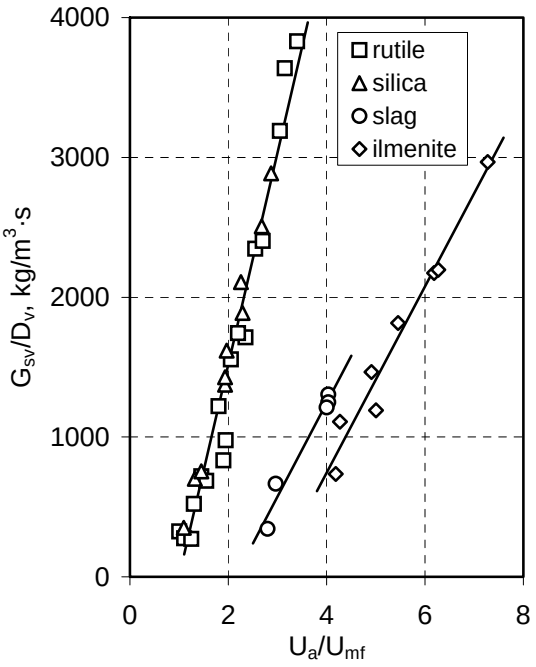

Figure 12. Relationship between the flow of solids in the L-valve and the aeration flow

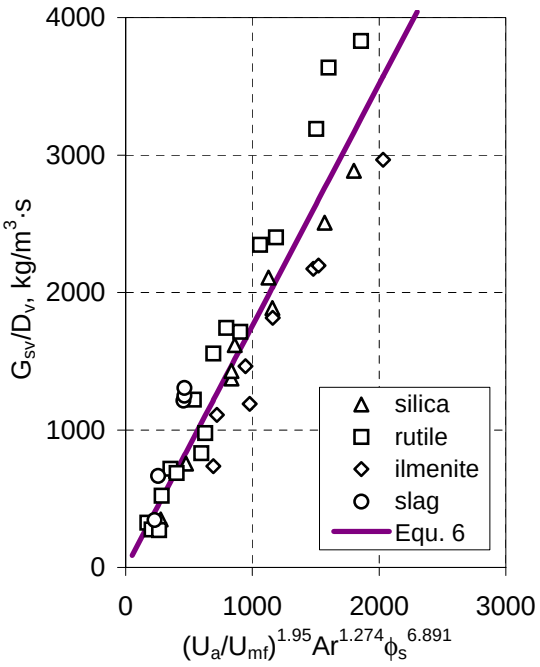

Figure 13. The correlation of solids flow in the L-valve

bulk density of the material:[14]

$$\frac{\Delta P_v}{L_v} = 0.0649\frac{G_{sv}^{0.178}\rho_b^{0.996}}{D_v^{0.574} d_p^{0.237}} \tag{9}$$

We ran through a similar exercise, but because the diameter of the L-valve remained fixed in our tests we could not properly include it as a variable. Our correlation took the form

$$\frac{\Delta P_v}{L_v} = 0.115\frac{G_{sv}^{0.137}}{\rho_b^{0.131} d_p^{0.64}} \tag{10}$$

which seems to relate a stronger dependence on particle size (stronger than the correlations in equation 8 and 9 suggest), but a weaker dependence on bulk density. The relationship between G_{sv} and ΔP_v certainly depends of the material tested (see Figure 14), and particle size and density are two properties that distinguish one material from another. The sample correlation

coefficient of equation 10 is 0.97 (see Figure 15). The average deviation between the correlation and the experimental data is 4.4%; the maximum deviation is 12%.

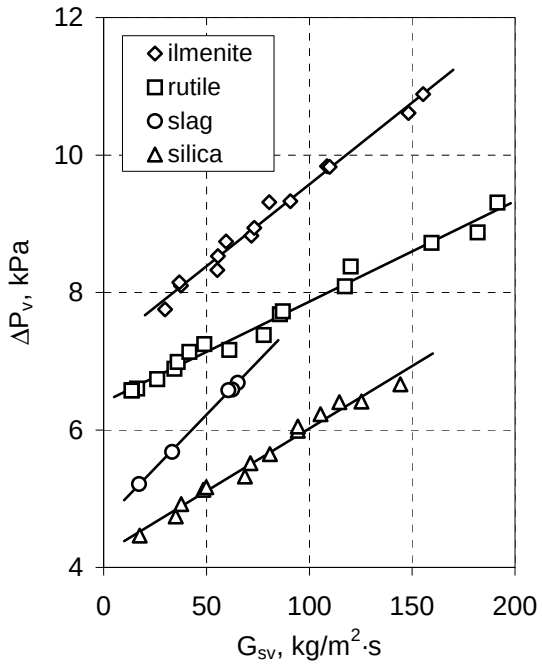

Figure 14. The relation between pressure drop across the L-valve and the solids flux through the valve

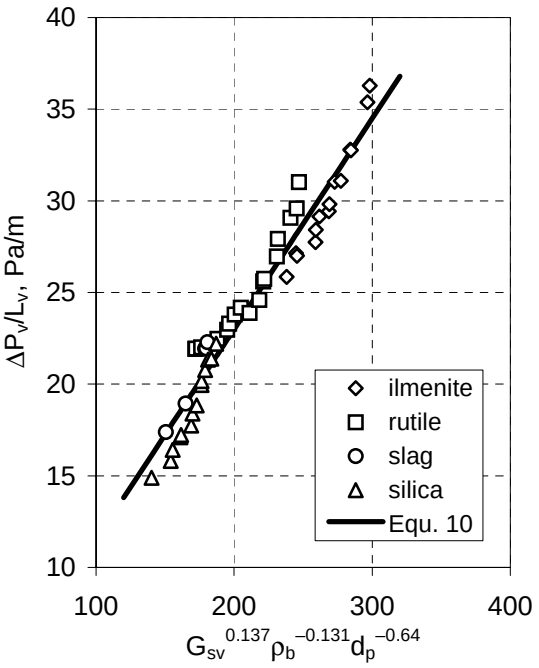

Figure 15. Pressure in the L-valve, correlated

CONCLUSIONS

Our study gives insights into the hydrodynamic behaviour of heavy minerals in a CFB. It also provides working relationships for controlling conditions in a CFB. From these insights and relationships we may draw conclusions about the operation of the CFB chlorinator:

1. A low aeration flow rate maintains stable circulation. Table 2 summarizes settings of the superficial aeration velocity for the four materials tested. Compare these values with velocities set in three chlorination trials towards the end of programme (February–March 2004): 0.4–0.6 m/s, 0.35–0.4 m/s, and 0.3 m/s. An order of magnitude sets the two groups apart. Aeration velocities in the chlorinator, even if they did approach the terminal velocity of the particles, were far above the minimum fluidizing velocity, and consequently fluidized solids in the standpipe and prevented the smooth movement of particles downwards. Slugs formed and moved up the column. Solids would have been expelled from the reactor through the primary cyclone—as we observed in the CFB chlorinator.
2. Stable fluidization in the cold model was concomitant with a substantial head of solids in the standpipe. From the position of the feeder ports about two-thirds of the way up the standpipe of the CFB chlorinator, we may conclude that the success of some tests might have been compromised by an insufficient head of solids in the standpipe.
3. Lower values of U and higher values of G_s are likely to improve chlorination reaction rates. These settings increase the residence time and total-solids holdup in the riser. Particles of ore and reductant, therefore, have longer to react and are in closer proximity to each other.
4. Slip velocities are independent of the solids-circulation flux in the riser, a conclusion that contradicts other findings reported in the literature.
5. The chlorinator may be run with relationships that we developed for the operation of the L-valve. Similar relationships reported in the literature under-estimate conditions and, therefore, do not apply.

6. Our results suggest that the operation of the L-valve is sensitive to the shape (or sphericity) of particles. Other studies worked with rounded particles and do not mention sphericity as an important factor.

NOTATION

Ar Archimedes number, dimensionless; Ar = $d_p^3(\rho_p - \rho)\rho g / \mu^2$
A_v cross-sectional area of the (L-valve) opening, m^2
d_p Sauter-mean particle diameter, m
d_{50} median particle size on the cumulative-percentage frequency curve, µm
$_{20}d_{80}$ range of particles sizes from d_{20} to d_{80}, µm
C_D discharge coefficient of the valve aperture, dimensionless
C_s solids concentration in a section of the riser, kg / m^3; $C_s = \rho_p(1-\varepsilon)$
D diameter of riser, m
D_v diameter of L-valve, m
g acceleration due to gravity, m / s^2
G_s solids circulation flux in the riser, kg / m^2·s
G_{sv} solids circulation flux in L-valve, kg / m^2·s
L_v length of the horizontal leg of the L-valve, m
P_i gauge pressure at port i of the CFB, kPa
Q_a volumetric flow of aeration gas, cm^3 / s
Re_{mf} Reynolds number at minimum fluidization, dimensionless; $Re_{mf} = U_{mf} d_p \rho/\mu$
U superficial gas velocity, m / s
U_a superficial velocity of aeration gas, m / s
U_{mf} minimum fluidizing velocity, m / s
U_{sl} slip velocity, m / s
U_t terminal velocity, m / s
W_s solids flow in the CFB, kg / s
z riser axial co-ordinate, m

Greek Letters

ΔP pressure drop between successive pressure ports, kPa
ΔP_r pressure drop across the riser, kPa
ΔP_v pressure drop across the L-valve, kPa
Δz distance between successive pressure ports, m
ε average voidage in a section of the riser, dimensionless
ε_{mf} voidage at minimum fluidizing velocity, dimensionless
ϕ_s sphericity, dimensionless
ρ gas density, kg / m^3
ρ_b bulk density, kg / m^3
ρ_p particle density, kg / m^3
μ gas viscosity, kg / m·s

ACKNOWLEDGEMENTS

Our thanks go to Melanie van Eck (North-West University) and Nigel Ramlall (University of KwaZulu-Natal) for their assistance in the test work. We are grateful to the (South African) Department of Science and Technology, through the Innovation Fund, for a grant (project No. 32211) that allowed us to construct the CFB.

REFERENCES

1. Luckos, A. and D. Mitchell (2002). The design of a circulating fluidized-bed chlorinator at Mintek. *In* A. Luckos and P. den Hoed (eds) *IFSA 2002, Industrial Fluidization South Africa:* 147–160. Johannesburg: S. Afr. Inst. Min. Metall.
2. Den Hoed, P., M.J. Freeman, A. Luckos and J. Nell (2003). An assessment of alternative processes for the production of TiO_2 pigments by chlorination. *Chem. Technol.* (September):27–30.

3. Nell, J. and P. den Hoed (2003). Carbochlorination of rutile, titania slag and ilmenite in a bubbling fluidized-bed reactor. In *IMPC 2003:* 1426–1433. Johannesburg: S. Afr. Inst. Min. Metall.
4. Davidson, J.F. (2000). Circulating fluidised bed hydrodynamics. *Powder Technol.* **113**:249–260.
5. Luckos, A. and P. den Hoed (2005). Pressure and solid distributions in the riser of a circulating fluidized bed. *In* K. Cen (ed.) *Circulating Fluidized Bed Technology VIII:* 231–238. Beijing: Int. Academic Publishers.
6. Luckos, A. and P. den Hoed (2004). Fluidization and flow regimes of titaniferous solids. *Ind. Eng. Chem. Res.* **43**:5645–5652.
7. Geldart, D. (1973). Types of gas fluidization. *Powder Technol.* **7**:185–195.
8. Kunii, D. and O. Levenspiel (1991). *Fluidization Engineering.* 2nd edition. Boston: Butterworth-Heinemann.
9. Yerushalmi, J. and A.A. Avidan (1985). High velocity fluidization. *In* J.F. Davidson, R. Clift and D. Harrison (eds) *Fluidization:* 225–291. 2nd edition. London: Academic Press.
10. Smolders, K. and J. Baeyens (1998). Hydrodynamic modeling of circulating fluidized beds. *Advanced Powder Technol*. **9**:17–38.
11. Geldart, D. and P. Jones (1991). The behaviour of L-valves with granular powders. *Powder Technol.* **67**:163–174.
12. Jones, D.R.M. and J.F. Davidson (1965). The flow of particles from a fluidized bed through an orifice. *Rheol. Acta* **4**:180–191.
13. Yang, W.-C. and T.M. Knowlton (1993). L-valve equations. *Powder Technol.* **77**:49–54.
14. Arena, U., C.B. Langeli and A. Cammarota (1998). L-valve behaviour with solids of different size and density. *Powder Technol.* **98**:231–240.